Bull. Soc. Photogr. Imag. Japan. (2025) Vol. 35 No. 2: 9–18

Original Paper

A Partial Image Processing Method with Full Reversibility for Smooth Boundary Representation

Yan ZHANG [a], Shoko IMAIZUMI [b]

Abstract: We propose a partial image processing for arbitrarily selected regions of interest (ROIs) with full reversibility. The main contribution of this paper is that the proposed method never causes artifacts around the ROIs by using a designed gradual boundary processing. Additionally, the original image can be completely restored from the processed image while preserving the file size before and after processing. To ensure reversibility, we embed the data necessary for restoration into the image itself after image processing, which results in the final processed image. The effectiveness of the proposed method is verified by evaluating the effects of partial image processing on the ROIs and assessing the influence of data embedding on visual quality.

Key words: image processing, reversibility, region of interest, boundary representation, file size preservation

1. Introduction

Recently, image-processing applications have become increasingly common with the development of devices with photo-editing capabilities and the expansion of cloud photo services. However, typical image-processing methods are irreversible; it is necessary to preserve either the source image or its editing history to revert to the original form of the image. The problem is that the size of the processed images increases. This requires more storage capacity, but the capacity of mobile devices is often limited.

Reversible data hiding (RDH)[1] is considered one of the most suitable technologies for solving these problems. RDH can restore an original image completely by extracting the embedded data and, in principle, maintains the file size before and after data hiding. Accordingly, image contrast enhancement (CE) methods with reversibility through RDH have been actively proposed. Typical image CE algorithms using RDH are based on a histogram shifting (HS) method[2]. This approach implements image CE while embedding recovery data in contrast-enhanced images. By including the recovery data in the processed image, the original form is completely recoverable. Subsequently, reversible image CE methods based on the method[2] have been developed to improve the effect. While numerous studies[2) -7)] have primarily focused on methods for grayscale images, color distortions may be introduced when directly applying them to color images. To cope with this issue, research on applying image processing to color images[8) -14)] is also evolving.

Wu et al.[8] proposed a novel method that enables lossless CE for color images. This method successfully achieved CE in color images with high-quality visual results, but in many cases, complete reversibility cannot be guaranteed. Addressing this issue, another method[10] was proposed that attained not only CE but also saturation improvement with full reversibility. An extended method[11] can further implement brightness increase/decrease, sharpening, and smoothing, in addition to CE and saturation improvement. Additionally, reversible color-tone control was developed in the method[12], which can control the coldness or warmth of an image.

These methods enable various image processing functions for color images, as well as CE, while ensuring reversibility and reducing saturation and hue distortion. With the exception of approaches for medical images[15) -17)], however, previous studies have predominantly focused on reversible image processing for the entire image, and limited consideration has been given to local processing methods for specific regions. Such local processing has attracted considerable attention in photo editing since it allows flexible adjustments to specific image regions and accommodates diverse and personalized editing requirements. Several studies[18),19)] have also explored the recognition and detection of regions of interest (ROIs). However, in these approaches[15) -19)], the ROIs are automatically determined by image segmentation algorithms, so users cannot arbitrarily define them. In addition, complete reversibility is not guaranteed, so the original image cannot always be fully restored. Notably, these methods are designed to handle only specific image formats, such as TIFF or BMP, in order to avoid irreversible compression. This approach is also adopted in this work.

In this paper, we propose a novel method that enables users to arbitrarily select ROIs and implements eight image processing func-

Received 4th September, 2025; Accepted 15th October, 2025; Published 14th November, 2025
[a] Graduate School of Science and Engineering, Chiba University
1-33 Yayoicho, Inage-ku, Chiba-shi, Chiba 263-8522, Japan
[b] Graduate School of informatics, Chiba University
1-33 Yayoicho, Inage-ku, Chiba-shi, Chiba 263-8522, Japan

(a) Original image
(red frame indicates ROI)

(b) Processed image with direct application for existing method

(c) Our goal

Fig. 1. Research challenge in partial processing (CE).

tions on selected ROIs. The main innovation of our method is that it attains partial image processing without noticeable boundaries between ROIs and non-ROIs (nROIs) under the condition of complete reversibility and file-size preservation before and after the entire processing. In our method, ROIs are defined as the regions subjected to processing and non-ROIs as the remaining areas. In Fig. 1, we provide a specific example of partial processing to clarify the challenge facing the method. As shown in Fig. 1 (b), a noticeable boundary can be seen when CE processing was applied to the ROI without considering boundaries. In contrast, we aim to represent the smooth boundary as shown in Fig. 1 (c) in this paper. Through our experiments, we demonstrate the effectiveness of the proposed method and evaluate the influence of embedding restoration data on the processed-image quality.

The rest of this paper is organized as follows. Section 2 presents related works on reversible image processing approaches for grayscale and color images. In Section 3, we propose a partial image processing method with full reversibility and describe the details of each step. Experiments for validating the effectiveness of the proposed method, including an evaluation of the visual quality and the influence of embedding restoration data, are demonstrated in Section 4. Finally, we conclude this paper in Section 5.

2. Related Works

2.1 Reversible Contrast Enhancement Methods for Grayscale Images

In recent years, many studies[3) -7)] have explored the use of RDH for CE in grayscale images. These studies typically implement reversible CE with HS-based RDH techniques. The most traditional method[2)] flattens the image histogram to enhance the contrast by embedding recovery data into the histogram. In this method, however, preprocessing causes noticeable distortion in some cases. The preprocessing is commonly used to avoid underflows or overflows of pixel values before CE. To cope with this issue, a novel method with extended preprocessing[5)] was proposed. The method reduces visual distortion by concatenating two bins under the use of adjacent bins.

While these methods may result in significant changes in the average brightness, several CE methods[4), 6), 7)] focus on brightness preservation. A two-dimensional histogram, which is generated by pairing two horizontally adjacent pixels, is used in the method[6)]. The two-dimensional histogram[7)] is further divided into two sub-histograms to effectively improve contrast and also preserve high visual quality. An effective method[3)] was further proposed to automatically determine the optimal enhancement intensity by setting a stop condition. As an application to medical images, another type of methods[15) -17)] use image segmentation algorithms to manually divide the images into ROIs and backgrounds and enhance only the contrast of the ROIs. All of the above methods, however, have been proposed for grayscale images. If these methods are applied directly to color images, color distortion might be caused.

2.2 Extensions for Color Images

To obtain the effects of image processing without color distortion, useful methods[8) -14)] have been proposed for color images. A reversible CE method[8)] introduced a HSV color model composed of hue (H), saturation (S), and value (V). Hereafter, value (V) is referred to as brightness in this paper. In this method, the hue and saturation components remain unchanged, while only the brightness component is modified. More precisely, the ratios among the RGB components are maintained, and histogram equalization is performed on the brightness component to achieve CE effects. However, rounding errors occur in the preservation of the hue component. This prevents the method from fully recovering the original image from the pro-

cessed image. Sugimoto et al.[11] proposed an extended method that ensures full reversibility by recording such rounding errors as recovery data. Additionally, this method enables multiple functions, such as saturation improvement, sharpening/smoothing, and brightness increase/decrease, in addition to CE, and gets better visual effects. An advanced RDH method[14] based on the HSV color model was proposed. This method enables automatic CE the same as the method[3] for grayscale images. It automatically enhances not only the contrast of the R, G, and B components but also that of the brightness component to further improve the visual quality. In another extension[12], red and blue color-tone control was further accomplished. In the method, correction coefficients are calculated in the YD_bD_r color space and multiplied by each pixel value, resulting in reversible enhancement of red or blue color tones.

2.3 Reversible Image Processing Method with Various Functions

The reversible image processing method[11] has a variety of functions and is the most relevant method to our method. Figure 2 illustrates the flow of the method. This method utilizes the HSV color model to attain brightness increase/decrease, sharpening/smoothing, CE, and saturation improvement reversibly. The conversion from RGB to HSV is simple, which helps reduce the size of recovery data. This conversion is formulated as

$$H = \begin{cases} 60 \times \frac{G-B}{Max-Min} & if \quad Max = R \\ 60 \times \left(\frac{B-R}{Max-Min} + 2\right) & if \quad Max = G \\ 60 \times \left(\frac{R-G}{Max-Min} + 4\right) & if \quad Max = B \\ undefined & Others, \end{cases} \quad (1)$$

$$S = Max - Min, \quad (2)$$

$$V = Max. \quad (3)$$

In Eq. (1), R, G, and B indicate the red, green, and blue values of a single pixel. Additionally, in those three equations, Max and Min refer to the maximum and minimum values among the R, G, and B components of a single pixel, respectively. In this method, a processing function is first implemented, and the hue component is then adjusted to reduce the color distortions caused by the processing. The necessary data for restoration is finally embedded into the image. Note that this method enables not only a single function but also multiple functions simultaneously. However, it processes the entire image uniformly and does not consider partial processing for only a part of the image. Such a technique has been especially required in the field of photo editing. In the next section, we propose a novel method that extracts a part of the image and allows partial processing with smooth boundaries.

3. Proposed Method

The main contribution of this paper is to provide partial processing in an image without causing artifacts at boundaries. As with the previous method[11], the proposed method achieves brightness increase/decrease, sharpening/smoothing, CE, and saturation improvement. The former five processing functions are applied to brightness, while the latter one is applied to saturation. In addition, our method enhances the red and blue color tones on the basis of the previous method[12]. Consequently, the proposed method can perform a total of eight different image processing functions on selected ROIs. Figure 3 presents the overall processing flow. Our method is divided into two main parts: ROI processing and restoration data embedding. In 3.1 and 3.2, we describe these two parts, respectively. The restoration processing is then explained in 3.3. We further discuss the advantages of the proposed method in 3.4.

3.1 ROI Processing

As illustrated in Fig. 3, the proposed method begins with the extraction of the ROI. The extracted ROI undergoes a processing function and is integrated with a nROI. For simplicity of explanation, this paper will proceed with an example of applying a single processing function to the extracted ROI, but it is also possible to combine multiple processing functions. The intermediate image obtained through this process does not contain the necessary data to restore the original image. The restoration data is thus embedded into the intermediate image using the prediction error expansion with histogram shifting (PEE-HS) method[20]. The detailed processes are given as follows.

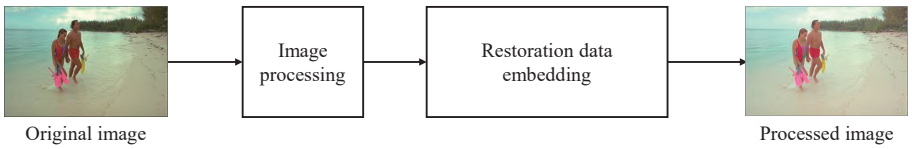

Fig. 2. Procedure of previous method[11].

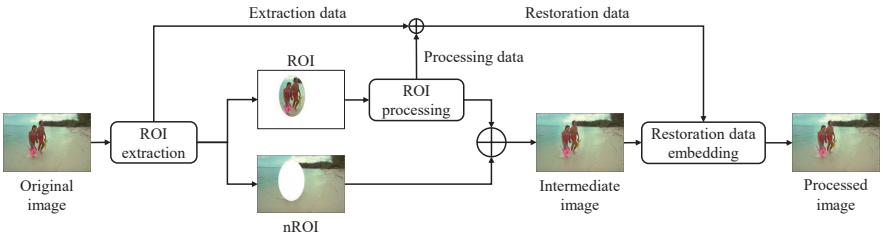

Fig. 3. Processing procedure of proposed method.

3.1.1 Extraction

Here, an arbitrary ROI is extracted. In the proposed method, we can also define multiple ROIs. The number of ROIs that can be selected depends on the embedding capacity, which varies with the characteristics of the image. Each ROI can be defined as either circular or rectangular, and we restrict ROI shapes to these two types in order to reduce the size of the recovery data. The extraction of rectangular and circular ROIs is explained in detail using Fig. 4. In the case that the target ROI is a rectangle, the three types of data given in Fig. 4 (a), namely the coordinates of the upper-left point (x_0, y_0), horizontal length a, and vertical length b, should be stored as restoration data. In the case that the target ROI is a circle, the three other types of data given in Fig. 4 (b), namely the center coordinates (x_0, y_0), horizontal radius a, and vertical radius b, should be stored.

3.1.2 Processing

Here, one of the eight processing functions is selected and applied to a single extracted ROI as an example. Similar to the previous method[11], the proposed method predefines the number of processing iterations to control the strength of the effect by the processing function. A preprocessing method[5] is used to avoid underflows or overflows before the main processing.

The primary contribution of this paper is the introduction of a gradual boundary processing method to address artifacts that appear along the ROI boundary. Figure 5 (a) shows the gradual boundary processing for a circular ROI. In this figure, the target processing region is gradually reduced until it overlaps with the ROI. Note that the initial target region is determined by the number of processing iterations and the interval m. The interval m, which prevents the appearance of artifacts at the ROI boundary, can be selected from positive integers depending on factors such as image size, image characteristics, and the number of processing iterations. It is specified to be the same in both horizontal and vertical directions to preserve the shape of the target region. No gradual boundary processing is carried out if $m = 0$.

While the target processing region is progressively reduced, the processing functions are repeatedly executed in the region. Consequently, the inner regions are subjected to a greater number of repetitions and are more strongly affected by the processing. Based on the above configuration, the proposed method can obtain a smooth boundary between the ROI and the nROI. The method also enables gradual boundary processing on nROIs. In this case, the ROI and nROI are inverted as shown in Fig. 5 (b).

The data necessary for restoration generated during the gradual boundary processing should be stored. Along with the data generated in 3.1.1, the data is embedded into the intermediate image.

3.2 Restoration Data Embedding

In the proposed method, the original image can be fully reconstructed by embedding the restoration data into the intermediate image. As illustrated in Fig. 3, the restoration data is composed of the ROI extraction data in 3.1.1 and the processing data in 3.1.2. The extraction data consists of a single bit to distinguish whether the processing region is ROI or nROI, another single bit to identify the shape of the ROI, and the three types of data described in 3.1.1. The processing data includes the type of processing function, the value of the interval m, the number of processing iterations, and the data resulting from gradual boundary processing. The processed image is finally derived by embedding the restoration data into the R, G, and B color components of the intermediate image using the PEE-HS method[20].

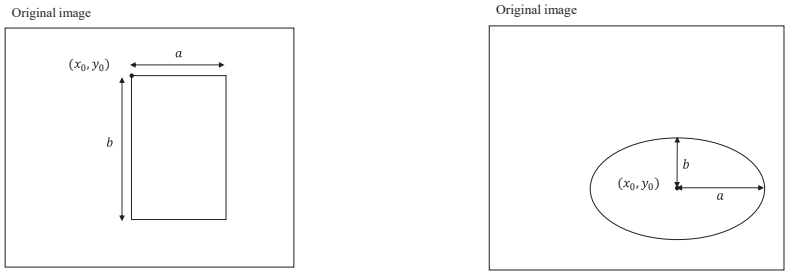

(a) Rectangular ROI (b) Circular ROI

Fig. 4. Extraction of ROI with different shapes.

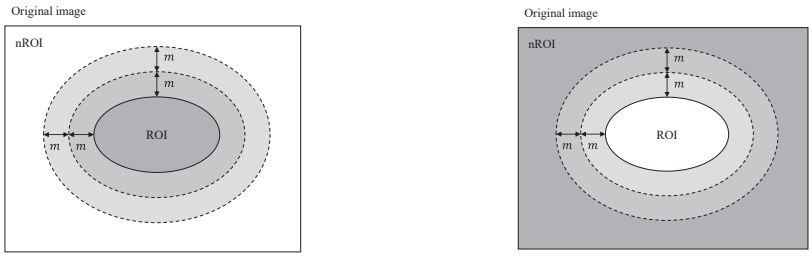

(a) ROI processing (b) nROI processing

Fig. 5. Gradual boundary processing of circular ROI.

3.3 Restoration Processing

The processed image can be fully reverted to its original form using the recovery data embedded into the image. Figure 6 displays the flow of the restoration process. The restoration data embedded in 3.2 is first extracted from each RGB component of the processed image. This process regenerates the restoration data and the intermediate image. Next, the ROI is identified on the basis of the ROI extraction data within the restoration data. The original ROI is then retrieved using the other restoration data, i.e., the processing data. We finally reconstruct the image with the original form by integrating the ROI with the nROI.

3.4 Advantages of Proposed Method

Our method enables reversible image processing on arbitrarily selected ROIs without causing boundary artifacts. The main advantages of the method are summarized as follows.

First, the proposed method allows users to select arbitrary rectangular or circular ROIs for the target processing region of reversible image processing. All of the previous methods process the entire image uniformly, whereas only the proposed method can process localized parts of the image. In addition, the region to be processed can be inverted from ROI to nROI.

Another main contribution is gradual boundary processing on the target processing region in order to smoothly represent the boundary between ROI and nROI. The gradual boundary processing delivers a smooth and effective processed image without creating any noticeable boundaries between the processed and non-processed regions.

As described above, the proposed method enables partial processing, which is not achievable in the previous methods. It further improves the flexibility and availability of reversible image processing and is expected to have a wider range of practical applications.

4. Experimental Results

We evaluated processed images obtained with the proposed method in terms of both image quality and reversibility. Twenty-four color images from the Kodak Lossless True Color Image Suite database[21] were used as test images. Each test image was downsampled to either 512 × 768 or 768 × 512 pixels using bicubic interpolation. In our experiments, the numbers of processing iterations were set to 30 for CE and brightness increase/decrease, 20 for saturation enhancement, and 2 for sharpening/smoothing. The interval parameter m was set to 1. For red or blue tone enhancement, the number of processing iterations was set to 15, with m = 3. It should be noted that the file size was identical before and after image processing in all experimental cases.

4.1 Evaluation Indices

We introduce multiple types of evaluation indices to quantitatively evaluate the image quality of the processed images. All of the following indices, with the exception of quality assessment, have been applied only to ROIs. First, we assessed the strength of the brightness increase/decrease by using the brightness difference between ROIs of both the original and processed images. The brightness value of each pixel within both ROIs was obtained using Eq. (3), and then the average of the brightness differences was calculated pixel-by-pixel. The sharpening and smoothing strengths were measured by the differences in the standard deviations of the brightness value of each pixel within the original ROI std_v and processed ROI std_v'. We explored the CE strength with the relative contrast error (RCE) [22]:

$$RCE = 0.5 + \frac{std_v' - std_v}{255}. \quad (4)$$

Note that RCE ranges from 0 to 1, and CE is observed in the case of $RCE > 0.5$. In addition, saturation improvement was evaluated on the basis of the difference in saturation between the ROIs of the

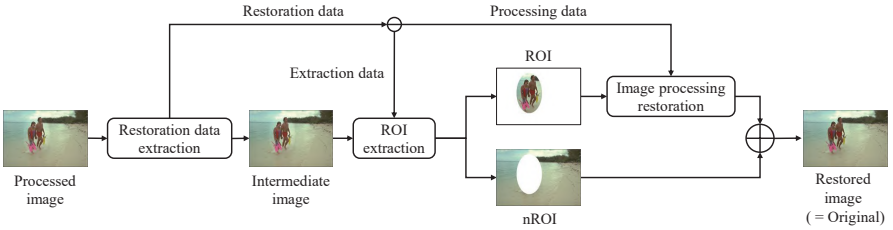

Fig. 6. Restoration procedure of proposed method.

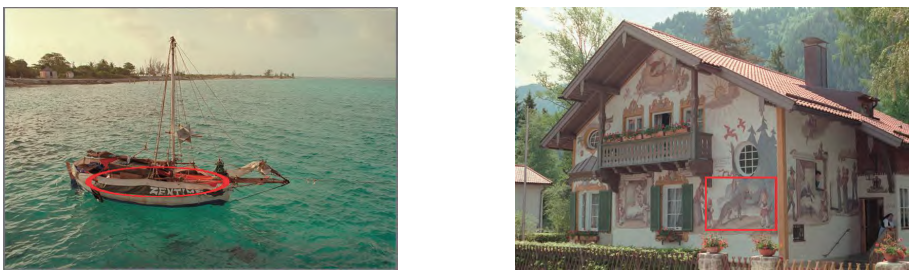

(a) kodim06 (circular ROI) (b) kodim24 (rectangular ROI)

Fig. 7. Example of single ROI extraction (red frames indicate ROIs).

original and processed images, where each saturation was calculated using Eq. (2). To assess the effectiveness of red or blue tone enhancement, we calculated the corresponding correction coefficient for the ROI: K_r for red tone enhancement and K_b for blue tone enhancement. A red tone enhancement is indicated when K_r>1, while K_b>1 denotes an enhancement in a blue tone. To verify the influence of data embedding, the quality between the intermediate and final processed images was assessed by using PSNR, SSIM[23] , and CIEDE2000[24].

4.2 Image Processing Effects for Single ROI

As can be seen in Fig. 7, as an example, we extracted a single circular ROI from kodim06 and a single rectangular ROI from kodim24. Note that each region surrounded by the red frame indicates the ROI, and image processing was only applied to the ROI in each image. First, we visually confirmed the processed images with each processing function. Figures 8 and 9 represent the processed images derived by the proposed method. In the ROIs in Figs. 8 (a), 8 (b), 9 (a), and 9 (b), where the brightness was increased or decreased, changes in brightness are clearly observed. Additionally, Figs. 8 (c), 8 (d), 9 (c), and 9 (d) demonstrate that the proposed method effectively sharpened or smoothed the extracted ROIs. The contrast of each ROI was effectively enhanced in Figs. 8 (e) and 9 (e). As shown in Figs. 8 (f) and 9 (f), the saturation within the ROI was successfully improved. Finally, Figs. 8 (g), 8 (h), 9 (g), and 9 (h) demonstrate that the proposed method effectively enhanced the red or blue tones within the ROIs. It is worth noting that the boundaries between ROIs and nROIs were smoothly represented by the gradual boundary processing in all the processed images. In contrast, Fig. 10 shows images processed without applying gradual boundary processing, that is, m = 0. As can be seen from this figure, noticeable boundaries were generated between ROI and nROI. Our method has provided a solution to avoid this issue.

To provide clearer visualization, we extracted and enlarged the

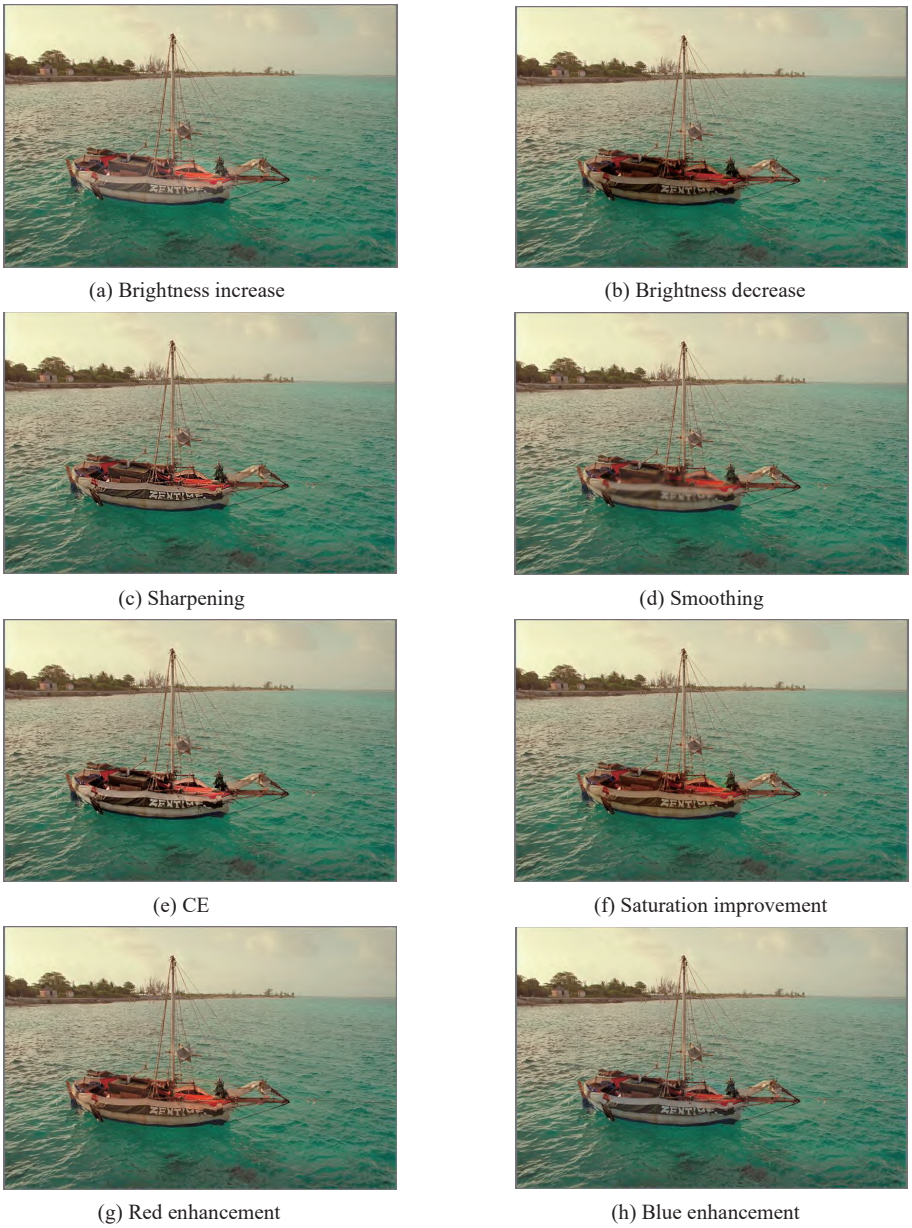

(a) Brightness increase (b) Brightness decrease

(c) Sharpening (d) Smoothing

(e) CE (f) Saturation improvement

(g) Red enhancement (h) Blue enhancement

Fig. 8. Image processing results for circular ROI.

ROIs along with their surrounding regions from two brightness-increased images processed with the proposed gradual boundary processing, as shown in Fig. 11. For comparison, the corresponding results obtained without gradual boundary processing are also presented. As illustrated in Figs. 11 (b) and 11 (e), the proposed method maintained the effectiveness of image processing while preventing noticeable boundaries.

Next, we quantitatively evaluated the processed images with each processing function. Table 1 shows the values of the evaluation indices for the test images. Note that each evaluation index was de-

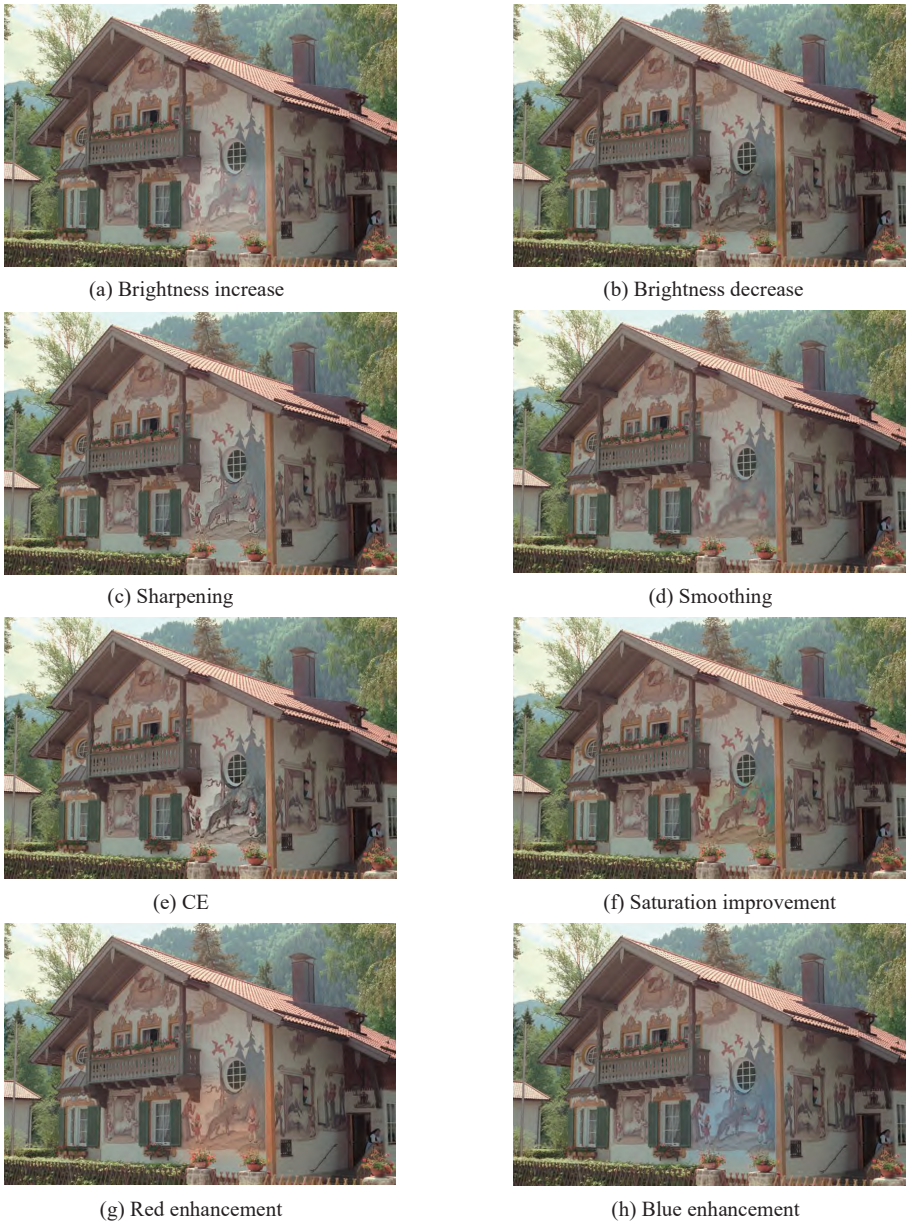

(a) Brightness increase (b) Brightness decrease

(c) Sharpening (d) Smoothing

(e) CE (f) Saturation improvement

(g) Red enhancement (h) Blue enhancement

Fig. 9. Image processing results for rectangular ROI.

Table 1. Effects of each processing function.

	Brightness difference		Standard deviation difference		RCE	Saturation difference	Correction coefficients	
	Brightness increase	Brightness decrease	Sharpening	Smoothing	CE	Saturation improvement	K_r (Red enhancement)	K_b (Blue enhancement)
kodim06 (circle)	30.98	-28.89	11.49	-7.73	0.5735	21.75	1.1176	1.1180
kodim24 (rectangle)	31.00	-29.00	3.64	-2.37	0.5743	22.00	1.1482	1.1474
Average	29.35	-27.68	6.18	-4.49	0.5614	19.91	1.1230	1.1309

(a) kodim06 (circular ROI) (b) kodim24 (rectangular ROI)

Fig. 10. Processed images with noticeable boundaries (m = 0).

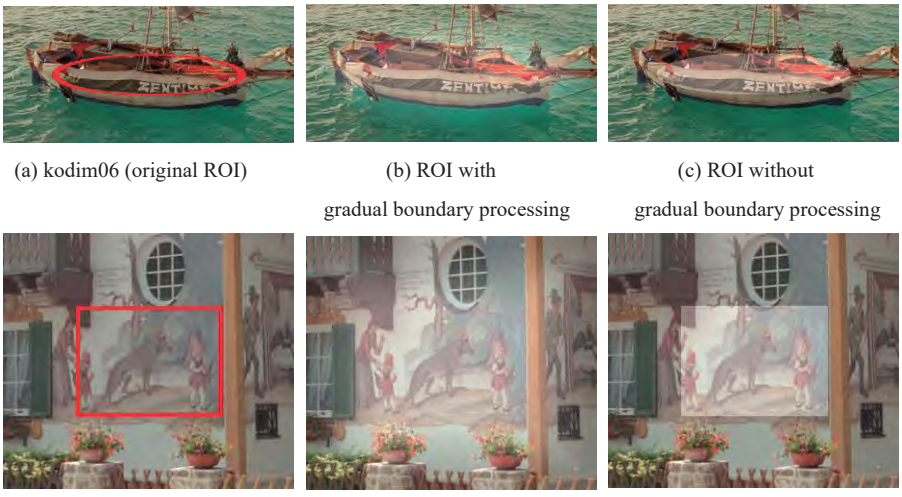

(a) kodim06 (original ROI) (b) ROI with gradual boundary processing (c) ROI without gradual boundary processing

(d) kodim24 (original ROI) (e) ROI with gradual boundary processing (f) ROI without gradual boundary processing

Fig. 11. Enlarged views of brightness-increased ROIs and their surrounding regions. Results with proposed gradual boundary processing are compared to those without it.

scribed in 4.1. In the case of brightness increase/decrease, the brightness differences properly exhibited positive values for increase and negative values for decrease. We then verified whether the sharpening and smoothing processing had been normally attained from the sign of each difference in standard deviations. With respect to the CE function, the RCE values exceeded 0.5 in both processed images. In addition, the saturation differences before and after the saturation improvement were positive. We calculated the average values of the whole dataset, and the results also demonstrated the effectiveness of each processing function.

To evaluate the effectiveness of the proposed gradual boundary processing, we computed the gradient magnitude of each pixel along the boundary regions and used their average as a measure of smoothness. The boundary region was defined by the outermost pixels within the ROI. The gradient magnitude was calculated as $|\nabla I|=\sqrt{(G_x^2+G_y^2)}$, where $|\nabla I|$ denotes the gradient magnitude, and G_x and G_y represent pixel gradients in the horizontal and vertical directions, respectively. These gradients were obtained using the central difference method. Table 2 summarizes the average gradient magnitudes for each test image under three conditions: the original, with the gradual boundary processing, and without the gradual boundary processing. For brightness adjustment, boundary smoothness was evaluated on the basis of the average gradient magnitude of brightness values within

Table 2. Average gradient magnitudes for evaluating effects of gradual boundary processing (GBP: gradual boundary processing, nGBP: non-gradual boundary processing).

		Average gradient magnitude		
		Original	**GBP**	**nGBP**
kodim06 (circle)	Brightness increase	23.79	23.88	40.45
	Brightness decrease		23.66	37.72
	Sharpening		37.65	45.34
	Smoothing		13.07	15.12
	CE		38.60	46.60
	Saturation improvement	15.64	21.24	44.84
	Red tone enhancement	22.65	26.14	33.74
	Blue tone enhancement	24.36	28.09	32.70
kodim24 (rectangle)	Brightness increase	20.12	20.48	29.95
	Brightness decrease		20.43	30.46
	Sharpening		22.82	24.94
	Smoothing		18.34	19.22
	CE		25.19	26.91
	Saturation improvement	21.82	29.60	40.70
	Red tone enhancement	18.20	20.83	23.25
	Blue tone enhancement	22.61	25.78	26.97

(a) Original image (red frames indicate ROIs) (b) Processed image

Fig. 12. Image processing results for multiple ROIs.

the boundary, while for other components, it was evaluated using the corresponding component values. Notably, the average gradient magnitudes obtained with the gradual boundary processing were closer to those of the original images. In contrast, those without the gradual boundary processing were significantly larger, which reflects reduced boundary smoothness.

Although only two images were used as examples, similar results were obtained for the other images. From the above visual confirmation and quantitative evaluation results, we clarified that the proposed method delivers effective processed images without causing artifacts at boundaries.

4.3 Image Processing Effects for Multiple ROIs

We further discuss the case of two circular ROIs selected from a single image as an example to verify the effectiveness of the proposed method for multiple ROIs. As illustrated in Fig. 12 (a), the extracted ROIs are depicted by the red frame, and different processing functions have been carried out for these ROIs. Figure 12 (b) shows the image processed under the condition that sharpening was applied to the left ROI and brightness increase was applied to the right one. The number of processing times for each function is as indicated at the beginning of Section 4.

From Fig. 12 (b), it is clear that the flower in the left ROI has been sharpened, and the brightness of the flower in the right ROI has increased. We can also observe that noticeable boundaries were not generated around both ROIs. In this way, the proposed method allows multiple ROIs to be selected independently, and a different processing function can be applied to each of these ROIs. Although we showed an example here, effective results were obtained by applying different processing functions to three or more ROIs using other test images. However, the proposed method is applicable to only non-overlapping ROIs at this point; discussion on application for overlapping ROIs is our future work.

Table 3. Image quality deterioration caused by data embedding.

		PSNR [dB]	SSIM	CIEDE2000
kodim06 (circle)	Brightness increase	68.07	0.9999	0.0297
	Brightness decrease	60.38	0.9997	0.0560
	Sharpening	63.04	0.9998	0.0372
	Smoothing	60.95	0.9996	0.0467
	CE	63.51	0.9999	0.0363
	Saturation improvement	65.77	0.9999	0.0312
	Red tone enhancement	78.19	0.9999	0.0245
	Blue tone enhancement	73.37	0.9999	0.0335
kodim24 (rectangle)	Brightness increase	63.09	0.9999	0.0391
	Brightness decrease	63.12	0.9999	0.0390
	Sharpening	61.77	0.9999	0.0406
	Smoothing	55.72	0.9994	0.1018
	CE	62.01	0.9999	0.0405
	Saturation improvement	63.12	0.9999	0.0390
	Red tone enhancement	63.58	0.9999	0.0226
	Blue tone enhancement	58.67	0.9999	0.0380

4.4 Influence of Data Embedding on Processed Image Quality

To guarantee reversibility, we embed the restoration data into the intermediate image. The data-embedding process commonly causes distortion in the processed image. We thus validated the influence of this process on the processed image quality. In this subsection, we focus on the case of a single ROI and evaluate the images shown in Figs. 8 and 9. Table 3 summarizes the PSNR, SSIM, and CIEDE2000 between the processed and intermediate images, namely the images before and after data embedding. The values of PSNR and SSIM were commonly high, and the values of CIEDE2000 were close to zero. These values indicated that the data-embedding process has little influence on the processed image quality.

The verification was performed on all of the 24 test images, and the results showed that there was very low influence on image quality for all of them. Figure 13 shows the results for all the images processed by the CE function, which had the lowest PSNR and SSIM values among all of the eight processing functions. Although there was some variation, the PSNR and SSIM values were above 50 dB and 0.994, respectively, for all the images. This indicates that the

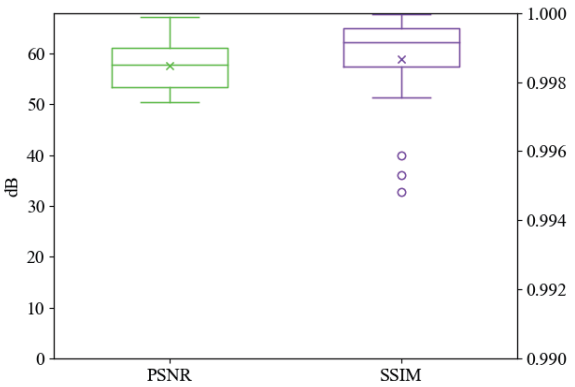

Fig. 13. Influence of data embedding on contrast-enhanced-image quality across all test images.

quality of each processed image was extremely high. These results revealed that the data-embedding process had little influence on the image quality of the processed images.

It is worth noting that we confirmed that the images restored from the processed images were fully consistent with their original forms in all cases. We calculated the PSNR and SSIM values between the original and restored images, which consistently resulted in PSNR = ∞ and SSIM = 1. Although numerous ROI-based image processing methods have been proposed, reversibility has not been considered in those methods.

In this experiment, the maximum amount of restoration data was approximately 40,000 bits. As described in 3.1.1, the maximum numbers of ROIs and processing times are determined in accordance with the embedding capacity. This design ensures that the restoration data always remain within the available embedding capacity of each image.

5. Conclusion

We proposed a reversible image processing method for regions of interest that does not cause artifacts at the boundaries. In the method, a single or multiple ROIs are first selected with either a circular or rectangular shape. Our method can represent smooth boundaries by gradually performing image processing on the ROIs. Further, in the case that multiple ROIs are selected, different processing functions can be applied to each of them.

Through our experiments, we clarified that each processing function is effective for the selected ROIs and that noticeable boundaries are not derived. We also confirmed that embedding the restoration data had little influence on the processed image quality and that reversibility can be guaranteed in all cases.

The method is currently applicable only to multiple ROIs that are apart from each other, not to overlapping ROIs. Our future work involves an extension for overlapping ROIs and an application to partial color-tone control.

References

1) Y.Q. Shi, X. Li, X. Zhang, H.T. Wu, and B. Ma, "Reversible data hiding: Advances in the past two decades," IEEE Access, vol.4, pp.3210–3237, 2016.
2) H.T. Wu, J.L. Dugelay, and Y.Q. Shi, "Reversible image data hiding with contrast enhancement," IEEE Sig. Process. Lett., vol.22, no.1, pp.81–85, 2015.
3) S. Kim, R. Lussi, X. Qu, and H.J. Kim, "Automatic contrast enhancement using reversible data hiding," IEEE International Workshop on Information Forensics and Security, Rome, Italy, 16-19, pp.1–5, November 2015.
4) S. Kim, R. Lussi, X. Qu, F. Huang, and H.J. Kim, "Reversible data hiding with automatic brightness preserving contrast enhancement," IEEE Trans. Circuits Syst. Video Technol., vol.29, no.8, pp.2271– 2284, 2019.
5) H.T. Wu, S. Tang, J. Huang, and Y.Q. Shi, "A novel reversible data hiding method with image contrast enhancement," Sig. Process. Image Commun., vol.62, pp.64–73, 2018.
6) H.T. Wu, X. Cao, R. Jia, and Y.M. Cheung, "Reversible data hiding with brightness preserving contrast enhancement by two-dimensional histogram modification," IEEE Trans. Circuits Syst. Video Technol., vol.32, no.11, pp.7605–7617, 2022.
7) Z. Bian, H. Yao, Y. Le, and C. Qin, "Two-dimensional histogram-based reversible contrast enhancement using bi-histogram equalization," Displays, vol.81, p.102580, 2024.
8) H.T. Wu, Y. Wu, Z. Guan, and Y.m. Cheung, "Lossless contrast enhancement of color images with reversible data hiding," Entropy, vol.21, no.9, p.910, 2019.
9) Z. Guan and H.T. Wu, "A reversible contrast enhancement scheme for color images," IEEE International Conference on Multimedia and Expo (ICME), London, UK, 6-10, pp.1–6, July 2020.
10) Y. Sugimoto and S. Imaizumi, "An extension of reversible image enhancement processing for saturation and brightness contrast," J. Imaging, vol.8, no.2, p.27, 2022.
11) Y. Sugimoto and S. Imaizumi, "Reversible image processing for color images with flexible control," Appl. Sci., vol.13, no.4, p.2297, 2023.
12) D. Nakaya and S. Imaizumi, "An extended method for reversible color tone control using data hiding," Electronics, vol.13, no.7, p.1204, 2024.
13) G. Gao, T. Han, B. Wu, J. Fu, and Z. Xia, "A hue preservation lossless contrast enhancement method with RDH for color images," Digit. Signal Process., vol.136, p.103965, 2023.
14) L. Han, Y. Ren, S. Tao, X. Zhang, and W. Gao, "Reversible data hiding with automatic contrast enhancement for color images," J. Vis. Commun. Image Represent., vol.101, p.104181, 2024.
15) H.T. Wu, J. Huang, and Y.Q. Shi, "A reversible data hiding method with contrast enhancement for medical images," J. Vis. Commun. Image Represent., vol.31, pp.146–153, 2015.
16) M. Shi, Y. Yang, J. Meng, and W. Zhang, "Reversible data hiding with enhancing contrast and preserving brightness in medical image," J. Inform. Secur. Appl., vol.70, p.103324, 2022.
17) Y. Yang, W. Zhang, D. Liang, and N. Yu, "A ROI-based high capacity reversible data hiding scheme with contrast enhancement for medical images," Multimed. Tools Appl., vol.77, no.14, pp.18043–18065, 2018.
18) J.L. Selvakani, B. Ranganathan, and G. Palanisamy, "A novel key point based ROI segmentation and image captioning using guidance information," Machine Vision and Applications, vol.35, no.6, p.127, 2024.
19) F. Ghezloo, O.H. Chang, S.R. Knezevich, K.C. Shaw, K.G. Thigpen, L.M. Reisch, L.G. Shapiro, and J.G. Elmore, "Robust ROI detection in whole slide images guided by pathologists' viewing patterns," Journal of Imaging Informatics in Medicine, vol.38, no.1, pp.439– 454, 2025.
20) D.M. Thodi and J.J. Rodriguez, "Expansion embedding techniques for reversible watermarking," IEEE Trans. Image Process., vol.16, no.3, pp.721–730, 2007.
21) "Kodak lossless true color image suite." Available online: http: //www.r0k.us/graphics/kodak/. (Accessed on 7 May 2025).
22) M.Z. Gao, Z.G. Wu, and L. Wang, "Comprehensive evaluation for HE based contrast enhancement techniques," Adv. Intell. Syst. Appl., vol.2, pp.331–338, 2013.
23) Z. Wang, A. Bovik, H. Sheikh, and E. Simoncelli, "Image quality assessment: from error visibility to structural similarity," IEEE Trans. Image Process., vol.13, no.4, pp.600–612, 2004.
24) G. Sharma, W. Wu, and E.N. Dalal, "The CIEDE2000 color-difference formula: Implementation notes, supplementary test data, and mathematical observations," Color Res., vol.30, no.1, pp.21–30, 2005.